Deformation Energetics of Chain Defects of Polyethylene

H. van der Werff, P. T. van Duynen,[†] and A. J. Pennings*

Laboratory of Polymer Chemistry, University of Groningen, Nijenborgh 16, 9747 AG Groningen, The Netherlands

Received August 2, 1989; Revised Manuscript Received November 27, 1989

ABSTRACT: The deformation energetics of static polyethylene chain defects were determined by means of molecular mechanics and energy minimization. The eight defects considered in our study were dispiration and dislocation (both interstitial- and vacancy-like), disclination, chain twist boundary (90° and 180°), and partial dislocation boundary. For these defects, energy minimized structures were calculated under action of tensile forces. It was found that one group of defects had moduli and deformation energetics identical with those of an all-trans chain, whereas the other group of defects had substantially lower moduli and a different deformation behavior. From the analysis of the distribution of deformation energy over the several degrees of freedom and by comparison to an all-trans chain, it could be concluded that defects inside a crystalline matrix are not weak links in polyethylene fibers. Weak links were concluded to be chains having higher moduli than the surrounding matrix (for example, taut tie molecules and especially entanglements in amorphous domains).

Introduction

The maximum tensile strengths of polymeric fibers obtained in practice are far below the corresponding theoretical strengths. For example, polyethylene fibers may be prepared having a tensile strength of more than 6 GPa,[1-3] whereas its theoretical strength can be estimated to be 33 GPa.[4-7] These results indicate the existence of features in polymeric fibers that severely limit the ultimate tensile properties and may arise from the complex interrelations between numerous factors: molecular weight of polymers, morphology of fibers, temperature, deformation rate, structure and properties of amorphous and crystalline domains, imperfect orientation, tie molecules, entanglements, tight knots, folds, flaws, voids, stress concentrations, residual stresses, crystal defects, etc. All these factors may have great influence on the failure mechanisms of fibers and have been evaluated extensively in an excellent review by Kausch.[8]

In this study, the deformation energetics of chain defects of polyethylene will be examined and compared to those of an all-trans chain. By doing this, insight is gained on how different chain conformations deform under tensile stress and how elastic energy is distributed over the degrees of freedom. Knowledge of these properties can be used to identify possible weak links in polymeric fibers.

Since the introduction of the Reneker defect,[9] several types of crystallographic defects have been reported: dispiration[9-11] and dislocation[12,13] (both insterstitial- and vacancy-like), disclination,[12] chain twist boundary (90° and 180°),[12] and partial dislocation boundary.[13] A summary of the properties of these defects is given by Reneker and Mazur.[13] In general, these defects may be involved in diffusion, translation, and rotation of molecules inside crystals, and they thus determine to a certain extent the physical properties of polymeric materials. Some studies have been reported on the tensile deformation of irregular chain conformations. McCullough et al.[14,15] have studied the energy deformation characteristics of primary units of tie molecules. Reneker and Mazur[16] have calculated static moduli of defects only for compressive forces as tensile forces gave numerically unstable calculations.

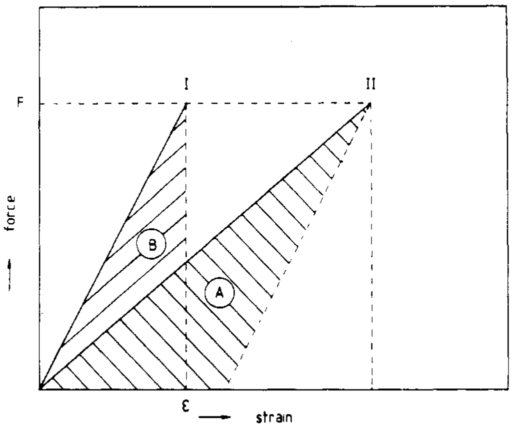

Figure 1. Force-strain curve of a high-modulus (I) and a low-modulus (II) chain. A: area proportional to the extra energy stored in II when both chains are stretched by force *F*. B: area proportional to the extra energy stored in I when both chains are drawn to strain ϵ.

The following considerations will illustrate the objective of our calculation. Suppose that two equally long chains have different elastic moduli. The force-strain curves of these chains are presented in Figure 1. Chain I has a higher modulus than chain II. If both chains are strained by the same tensile force, the low-modulus chain II will have stored more elastic energy in its chain than chain I. This extra energy in chain II relative to chain I at force *F* is proportional to area A in Figure 1. If both chains are drawn to the same strain ϵ, the high-modulus chain I has stored the largest amount of elastic energy, and this extra energy relative to chain II is proportional to area B in Figure 1. So at the same force or strain level, chains having different elastic moduli may have absorbed very different amounts of potential energy. These energies may be stored in bonds, bond angles, etc.

The purpose of this study is to investigate the influence of the structure of a polymer chain on the deformation behavior. By analyzing the distribution of deformation energy of various different chain structures over the degrees of freedom, one might identify structures that concentrate more energy into bonds than others.

Computational Details

Molecular mechanics calculations were carried out with the Groningen Molecular Simulation (GROMOS) computer

---

* To whom correspondence should be addressed.

[†] Laboratory of Chemical Physics, University of Groningen, Nijenborgh 16, 9747 AG Groningen, The Netherlands.

0024-9297/90/2223-2935$02.50/0

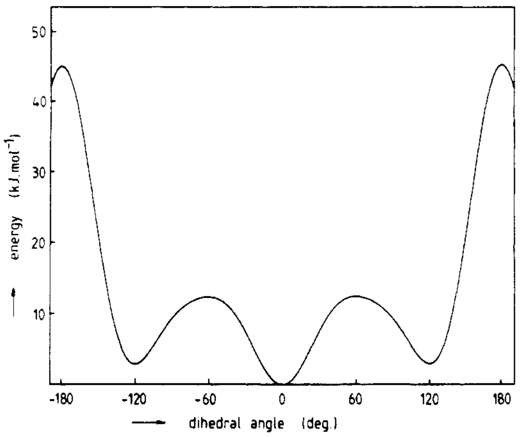

Figure 2. Ryckaert–Bellemans dihedral angle potential function using the parameters mentioned in the text.

program package, written by van Gunsteren and Berendsen.[17] This versatile package has been developed for the dynamic modeling of (bio)molecules and contains programs on molecular dynamics, stochastic dynamics, energy minimization, and analysis of molecular conformations.

In our calculations we considered single chains consisting of 19 backbone (carbon) atoms. Hydrogen atoms and therefore all related interactions were omitted.

The covalent bond stretching potential used was

$$V_b = \frac{1}{2}\sum_{i=1}^{N-1} k_b(b_i - b_0)^2 \tag{1}$$

where N is the number of atoms. The equilibrium value of the C–C bond length, b_0, was taken to be 0.153 nm with $k_b = 2.65 \times 10^5$ kJ·mol^{-1}·nm^{-2}.[18] The bond angle bending potential was also taken as a harmonic function

$$V_\Theta = \frac{1}{2}\sum_{i=1}^{N-2} k_\Theta(\Theta_i - \Theta_0)^2 \tag{2}$$

where $k_\Theta = 520$ kJ·mol^{-1}·rad^{-2} was derived from a potential used by Weber.[19,20] The equilibrium value of C–C–C bond angle was taken to be 111.0°. Because intramolecular nonbonded interactions were not taken into account explicitly, it was convenient to use the Ryckaert–Bellemans potential function[21,22] for dihedral angles:

$$V_\Phi = \sum_{i=1}^{N-3}\left(\sum_{n=0}^{5} C_n(\cos \Phi_i)^n\right) \tag{3}$$

with $C_0 = 9.2789$, $C_1 = 12.1557$, $C_2 = -13.1201$, $C_3 = -3.0597$, $C_4 = 26.2403$, and $C_5 = -13.4950$. The values of these parameters correspond to a trans–gauche energy barrier of 12.3 kJ·mol^{-1} and to an energy of the gauche minimum of 2.9 kJ·mol^{-1}. The dihedral angle potential function is displayed in Figure 2.

Due to the fact that we only considered single chains in our calculations, it was necessary to constrain the chain structure, because otherwise every chain conformation would transform back into an ordinary all-trans chain during energy minimization. In order to prevent this, each defect conformation of a single chain was preserved during tensile deformation by applying a dihedral angle restraining potential:[23]

$$V_\Phi^{\text{restr}} = \sum_{i=1}^{N-3}\left(k_\Phi^{\text{restr}}\{1 + \cos(\Phi_i - \delta_i)\}\right) \tag{4}$$

By choosing a specific set of phase shifts δ_i for a given chain conformation and an appropriate value of the dihedral angle restraining force constant k_Φ^{restr}, one can preserve with this restraining potential the specific conformation of a chain during energy minimization and thus examine differences in deformation energetics caused by differences in chain conformations.

Table I
Sequences of Carbon Atoms Used in This Study from the Structures of Chain Defects Reported by Reneker and Mazur[13]

defect name	no.	sequence
interstitial-like dislocation	1	C_{22}–C_{40}
interstitial-like dispiration	2	C_{20}–C_{38}
disclination	3	C_{21}–C_{39}
partial dislocation boundary	4	C_{23}–C_{41}
vacancy-like dislocation	5	C_{22}–C_{40}
vacancy-like dispiration	6	C_{23}–C_{41}
chain twist boundary (90°)	7	C_{22}–C_{40}
chain twist boundary (180°)	8	C_{19}–C_{37}

In this way, one can determine directly the influence of a certain conformation on the deformation behavior. In reality, a specific conformation is constrained by its surroundings, and deformation probably is accompanied by conformational changes that depend strongly upon the nature of the neighboring chains and the potential exerted by them. Of course, these phenomena are not modeled by the dihedral angle restraining potential. Application of this potential, which fixes a given conformation, only enables one to examine tensile properties of a static chain conformation for relatively small deformations. The potential only mimics the effect of a neighboring chain with respect to the fact that it provides the potential energy well that has that specific chain conformation at its energy minimum. The examination of possible large conformational rearrangements during deformation is therefore beyond the scope of the present investigation.

The restraining force constant k_Φ^{restr} was taken to be 500 kJ·mol^{-1}, which proved to be just large enough to prevent transitions of the dihedral angles during deformation. In using significantly higher values of k_Φ^{restr}, we found that the energy minimization algorithms gave unstable results. The stretching of a chain was accomplished by applying equal but oppositely directed tensile forces on the first and last atoms of the chain. The tensile forces were directed along the line connecting the first and last atoms and were kept constant during a single stretching event.

Energy minimization was carried out by the subsequent application of two methods: steepest descents and conjugate gradients.[24] Both are gradient methods, requiring function and derivative values. The steepest descents method[25] performs well far from a minimum but converges slowly near a minimum or when searching in a long, thin, curving valley. The conjugate gradients method[26] searches along directions corresponding to the local quadratic approximation of the function and usually converges superlinearly.

The initial structures of the various chain defects were taken from results of Reneker and Mazur.[13] They have published coordinates of chain defects of about 60 carbons long. Out of these chains, we picked a sequence of 19 carbon atoms encompassing the entire defect region. The sequences are listed for every chain defect in Table I. For sake of brevity, each defect is given a number in Table I, and this numbering will be used throughout the rest of the text.

The deformation process was executed as follows. At first, sets of phase shifts δ_i to be used in the dihedral angle restraining potential were calculated from the orig-

Table II
Length L_0, Bond Energy V_b, Bond Angle Energy V_Θ, Dihedral Angle Energy V_Φ, and Dihedral Angle Restraining Energy V_Φ^{restr} of the Initial Structures of the Various Chain Defects (See Table I) and an All-Trans Chain

defect no.	L_0, nm	V_b, kJ·mol^{-1}	V_Θ, kJ·mol^{-1}	V_Φ, kJ·mol^{-1}	V_Φ^{restr}, kJ·mol^{-1}
1	2.034	0.0	0.3	65.4	3.6
2	2.135	0.1	0.1	36.6	2.1
3	2.154	0.0	0.2	40.5	2.6
4	2.181	0.0	0.0	11.0	0.6
5	2.270	0.0	0.0	0.0	0.1
6	2.268	0.0	0.0	23.0	2.7
7	2.268	0.0	0.0	14.9	1.4
8	2.263	0.0	0.0	35.7	2.6
all-trans	2.270	0.0	0.0	0.0	0.0

inal conformation as reported in ref 13. The chains were energy minimized to give starting conformations by applying all the potentials except the tensile forces. The force–strain curves were calculated by applying a set of tensile forces that increased by small increments and energy minimizing the strained chain structure after each increment. The increment of the tensile force was taken to be 8.3×10^{-11} N, and the tensile force was incremented 20 times up to 1.66×10^{-9} N. All calculations were performed in single precision on a VAX 11/750 machine.

We also performed similar calculations on deformation of the same chain defects, taking into account hydrogen atoms and all related bond and bond angle interactions, as well as explicit nonbonded interactions and neighboring chains. However, we found that under stress these systems could not be brought into a stable energy minimum. These calculations produced slightly curved potential energy surfaces in which the total energy decreased negligibly and several degrees of freedom changed drastically.

Similar problems were also encountered by Reneker and Mazur.[16] As our primary interest was in the deformation energetics with respect to bonds and bond angles, we chose the simpler model described above.

Results

Table II lists the length and various energies of the energy-minimized chain defects to be used as starting structures for the tensile deformation calculations. The defects 1–4 are ca. 4–10% shorter than an all-trans chain, whereas the defects 5–8 are nearly equally long. The energy stored in the dihedral angles for most defects is considerable, and the dihedral angle restraining energy is quite low. All defects have virtually no bond and bond angle energy. This means that the initial structures are laxed with respect to bond and bond angles and thus allow the differences in deformation energetics, caused by differences in chain conformation, to be examined.

The results of the tensile deformation calculation will be presented in the following by the comparison of the deformation behavior of two chain structures that gave the most different results. Conclusions from this comparison proved to be general for all the chain structures considered in our study. The force–strain curves for an all-trans chain and a dislocation interstitial-like (defect 1) are given in Figure 3.

Because the initial lengths of these two chain structures differ less than 10%, no serious error is introduced by using strain instead of displacement on the x axis, especially when the differences in deformation behavior are as large as in Figure 3. The force–strain curves in Figure 3 are reasonably linear. If one assumes the cross section per chain in a polyethylene unit cell to be 18.3 Å^2, the elastic modulus of the all-trans chain from Figure 3 would be 177 GPa.

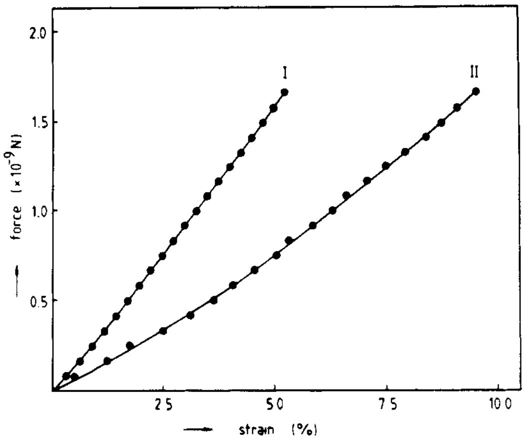

Figure 3. Calculated force–strain curves for an all-trans chain (I) and an interstitial-like dislocation (II).

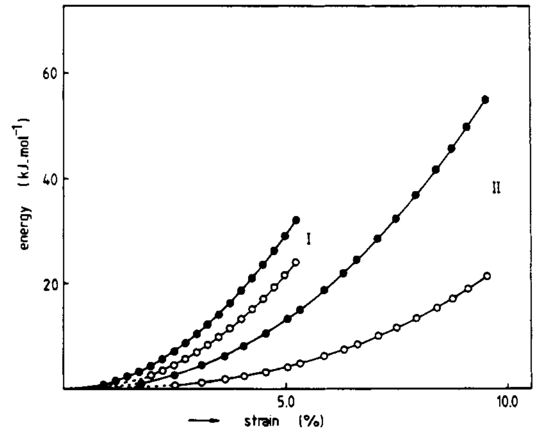

Figure 4. Bond energy V_b (○) and bond angle energy V_Θ (●) versus strain for an all-trans chain (I) and an interstitial-like dislocation (II).

There is considerable ambiguity about the ultimate value of the Young's modulus of polyethylene. Theoretical values from molecular mechanics calculations have been reported ranging from 186 GPa[27] to 267 GPa[7] to 380 GPa.[15] Experimental estimates have been reported by means of X-ray diffraction (240 GPa[28]), neutron scattering (329 GPa[29]), Raman scattering (358 GPa[30]), and stress–strain measurements (288 GPa[31]). In a recent evaluation of these results by Fanconi and Rabolt,[32] it was concluded that data from neutron and Raman scattering give the better estimates of the ultimate values of the Young's modulus.

It must be concluded, therefore, that the potentials and force constants in this study yield too low absolute values for the elastic modulus. This, however, does not give rise to serious problems, because we are mainly interested in the differences in deformation energetics of various chain conformations and not in the independent, absolute values of properties of each conformation.

The modulus of defect 1, 98 GPa (Figure 3), is much lower than that of the all-trans chain and has absorbed more energy during deformation. In Figure 4 bond energy V_b and bond angle energy V_Θ are plotted versus tensile strain for the same chains as in Figure 3. Both structures have been strained up to a tensile force of 1.66×10^{-9} N. The deformation of an all-trans chain causes a synchronous rise in bond and bond angle energies, although the latter rises more steeply. Qualitatively, the same holds for the low-modulus defect 1, but the bond angle energy rises more steeply with respect to the bond energy during deformation than in case of the all-trans chain. At a given strain, both the bond and bond angle energies of the low-modulus defect 1 are much lower than the corresponding energies of an all-trans chain. At the maximum tensile force, the ratio V_b/V_Θ is 0.75 for the all-trans chain and 0.39 for defect 1. Thus the low-modulus chain defect stores relatively less energy in bonds during deformation, but Figure 4 also shows that the absolute amount of energy stored in bonds is nearly the same as in case of the all-trans chain and that the absolute amount of bond angle energy is consequently higher.

From the results presented in Figure 4, it can be concluded that low-modulus chain defects placed in an all-trans matrix, for example a defect inside a crystalline domain, are under no conditions weak links in polyethylene fibers. When the matrix and the defect inside it are strained to a certain amount, the matrix chains will have stored much more energy in bonds than the chain defect.

In contrast to this, all-trans chains inside a defect matrix, for example taut tie molecules inside an amorphous domain or tie molecules in a defect boundary between crystalline domains, certainly are likely points for chain breaking, for they are subjected to high strains, due to the low modulus of the matrix, and have much more energy stored in bonds at a given strain. These results indicate that the morphology of a fiber causes certain chains to be weak links. This is in good agreement with fiber models as proposed by Peterlin,[33] which may already explain the general macroscopic mechanical properties of polymeric fibers.[34]

It should be noted that in our calculations, defects are assumed to be static structures. Diffusion and translation of a defect[13] under tensile stress could not be taken into account, although these phenomena might cause, for example, easy pull out of chain defects from crystalline domains and thus might have considerable consequences on the tensile properties of fibers.

The bond and bond angle energies of the two chains are plotted versus the tensile force in Figure 5. Figure 5 shows that at a given tensile force the bond angle energy V_Θ stored in the low-modulus defect is much higher than for an all-trans chain and that bond energies at a given tensile force are nearly equal for both chain structures, although the bond energy in an all-trans chain is systematically slightly higher. These results indicate that, if one considers low-modulus chain defects connected in series with all-trans chains, chain defects are not weak links. Although these defects are subject to larger strains at a given tensile force and have taken up more elastic energy during deformation than all-trans chains, the distribution of the deformation energy is such that, in absolute values, this is stored in bond angles and as equal energy in bonds.

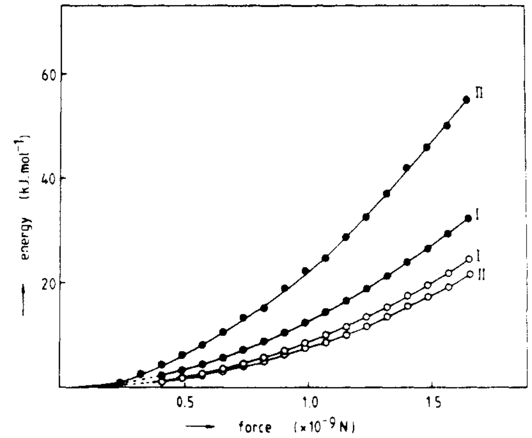

Figure 5. Bond energy V_b (○) and bond angle energy V_Θ (●) versus tensile force for an all-trans chain (I) and an interstitial-like dislocation (II).

The results on all chain defects and an all-trans chain are summarized in Table III. In general, two types of chain defects could be distinguished: chain defects with a modulus substantially lower (25–40%) than that of an all-trans chain (defects 1–4), and chain defects with a modulus nearly equal (within 2%) to that of an all-trans chain (defects 5–8). The differences in deformation energetics of the two groups are qualitatively similar to differences outlined in Figures 3–5. Table III shows that changes in V_Φ and V_Φ^{restr} during deformation are generally very small as compared to changes in V_b and V_Θ.

In Figures 6 and 7, stereodrawings are presented of chain structures at rest, with no tensile force acting, and structures at maximum tensile force. In Figure 6 structures are shown of an interstitial-like dislocation (defect 1), i.e., a low-modulus defect, and Figure 7 shows structures of a chain twist boundary (180°) (defect 8), which has a deformation energetics similar to that of an all-trans chain. From Figures 6 and 7 it is clear that the specific chain structures of the defects have been preserved during deformation by applying the dihedral angle restraining potential and that the conformation of the chains with respect to dihedral angles is very different, leading to differences in deformation energetics, as has been shown in the preceding sections.

Discussion

Chains carrying the load within amorphous domains and interconnecting crystalline domains are systematical weak links because they are subjected to relatively high strains due to the much lower modulus of their surrounding matrix and the concentration of stress on these chains.

It has been argued that entanglements play a major role in the interconnection of crystalline blocks through

Table III
Total Energy Change $\Delta V_{\mathrm{total}}$ and Changes in Bond Energy V_b, Bond Angle Energy V_Θ, Dihedral Angle Energy V_Φ, Dihedral Angle Restraining Energy V_Φ^{restr} and Tensile Strain ϵ at the Maximum Tensile Force of 1.66 × 10^{-9} N, and Modulus E of the Various Chain Defects (See Table I) and an All-Trans Chain

defect no.	$\Delta V_{\mathrm{total}}$, kJ·mol^{-1}	ΔV_b, kJ·mol^{-1}	ΔV_Θ, kJ·mol^{-1}	ΔV_Φ, kJ·mol^{-1}	$\Delta V_\Phi^{\mathrm{restr}}$, kJ·mol^{-1}	ϵ, %	E, ×10^{-8} N
1	86.6	21.8	55.8	6.1	3.0	9.55	1.79
2	73.4	23.3	47.2	1.4	1.4	9.18	2.23
3	70.4	23.2	42.4	5.1	−0.2	7.54	2.29
4	72.1	24.2	45.6	1.7	0.7	7.05	2.44
5	56.4	24.2	32.2	0.0	0.0	5.20	3.18
6	57.6	24.6	33.0	−0.8	0.9	5.24	3.23
7	57.8	24.7	33.1	−0.5	0.6	5.24	3.18
8	58.1	24.5	33.3	−1.0	1.3	5.28	3.18
all-trans	57.4	24.7	32.7	0.0	0.0	5.25	3.24

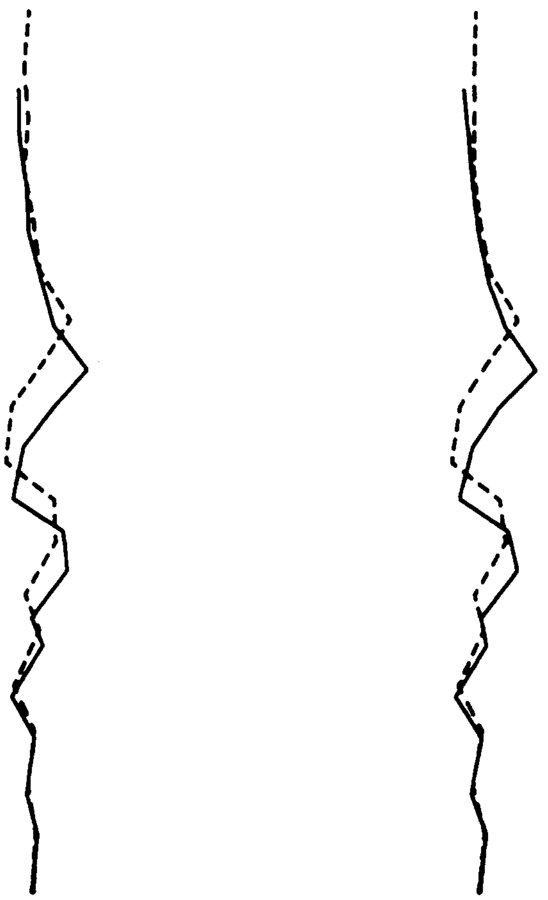

Figure 6. Superimposed stereodrawings of an interstitial-like dislocation at rest (solid lines) and at a tensile force of 1.66 × 10^{-9} N (broken lines).

amorphous regions. Flory and Yoon concluded that neighboring crystal lamellae grown from the melt are profusely interconnected not only by tie chains from one lamella entering another but also by entanglements involving chains reentering the same lamellae after passing through the amorphous region.[35]

They noted that entanglements cannot disappear during crystallization and are concentrated in the amorphous regions for they are preferentially excluded from the crystalline lamellae. Lacher et al.[36] have accumulated evidence, by means of computer simulations, that seems to indicate that indeed entanglements are a major contribution to the interconnection of crystalline lamellae.

In the gel-spinning process of polyethylene,[3,37] dilute polymer–solvent gels are spun to give fibers that, after extraction of the solvent, consist of lamellae interconnected by entanglements and that are hot-drawable to a certain maximum draw ratio λ_{max}. For more dilute gels, the molecular weight between entanglements is increased (i.e., a reduction of the number of entanglements per volume after extraction of the fiber). Consequently, higher maximum draw ratios can be achieved. At λ_{max}, the tensile strength depends drastically upon the number of entanglements per unit volume. For example, a gel-spun and hot-drawn fiber from a 5 wt % polyethylene/paraffin oil gel has a tensile strength at λ_{max} of 4 GPa,[3] whereas an identical fiber from a 1.5 wt % gel has a tensile strength of 7.2 GPa at λ_{max}.[38] Hot-drawn fibers from melt-spun polyethylene, i.e., fibers with a low molecular weight between entanglements, have much lower tensile strengths.

Arguments in favor of the assumption that entanglements as well as taut tie molecules are responsible for the stress transfer in gel-spun and consecutively hot-drawn polyethylene fibers have been reported,[39] deduced from results of annealing,[40] crazing,[41] electron beam irradiation,[42] and fracture experiments.[43] From the results of this study and the preceding arguments, it can be concluded that load-carrying entanglements inside amorphous domains are likely points for chain breaking in polymeric fibers, due to the fact that they are embedded in a low-modulus region that does not contribute to the interconnection of neighboring crystalline domains.

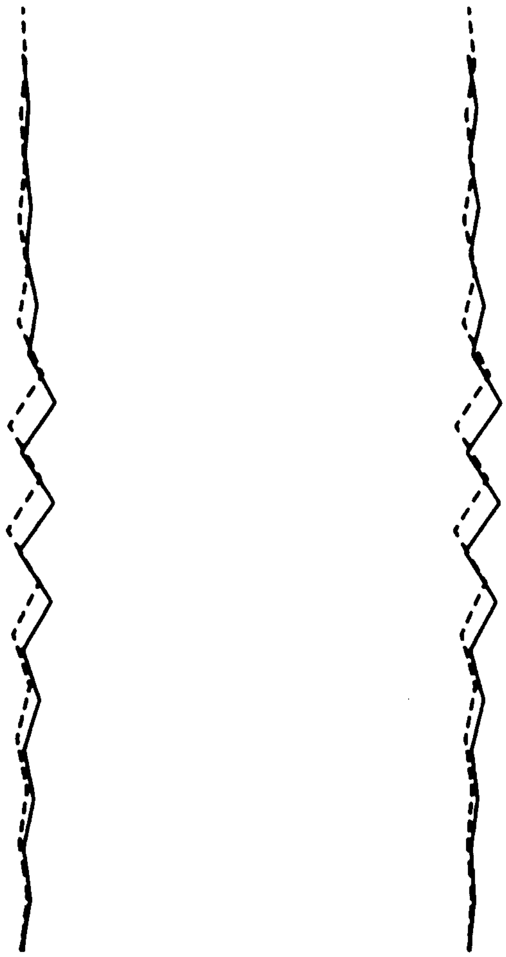

Figure 7. Superimposed stereodrawings of a chain twist boundary (180°) at rest (solid lines) and at a tensile force of 1.66 × 10^{-9} N (broken lines).

Particularly, entanglements will have a high modulus, because tensile deformation will bring two chains in very close contact, causing a dramatic rise of the repulsive forces and chain scission at an earlier strain. Chain-end radicals thus formed may initiate a mechanochemical chain reaction after Zakrevskii and Zhurkov[44] and lead to submicrocracks.

It needs to be stressed that creep may also play an important role in the failure process of gel-spun polyethylene fibers. It has been shown that under certain conditions the tensile strength of polyethylene fibers is determined by a stress-induced orthorhombic–hexagonal phase transition.[43] In the hexagonal phase chains can easily slip past one another, thus causing creep failure of the fiber. This phase transition obviously depends on the strength of the lateral interactions between the polymer chains. Thus fibers from rigid-rod polymers such as poly(*p*-phenyleneterephthalamide), which do have strong lateral interactions in the crystal lattice due to hydrogen bonding, may already exhibit tensile strengths of 3.4 GPa at a molecular weight of 2 × 10^4.[45] In the case of polyethylene, molecular weights of at least 2 orders of magnitude higher are required to reach comparable tensile strengths.

Conclusions

The deformation energetics of various static chain defects were determined. Two types of chain defects could be distinguished: low-modulus defects and defects closely resembling all-trans chains. From a study of the distribution of the elastic energy during deformation over bonds and bond angles, it was concluded that chain defects embedded in an all-trans chain matrix or connected to all-trans chains are not weak links and that high-modulus chains inside a low-modulus chain matrix certainly are likely to break first.

From this it can be concluded that chain defects inside crystalline domains or along a given chain molecule are not the chains in polymeric fibers that break first. The "weak links" are a larger scale aspect of the morphology. Taut tie molecules and especially entanglements, wherever they are, will be the first to break during the deformation process, leading to the macroscopic brittle failure of the fiber, whereas disentangling of the network via the hexagonal phase leads to ductile fracture.

Acknowledgment. This study was supported by the Netherlands Foundation of Chemical Research (SON) with financial aid from the Netherlands Organization for the Advancement of Pure Research (NWO) and AKZO, The Netherlands.

References and Notes

(1) Savitskii, A. V.; Gorshkova, I. A.; Shmikk, G. N.; Frolova, I. L. *Vysokomol. Soedin., Ser. B* **1983**, *25*, 352.
(2) Savitskii, A. V.; Gorshkova, I. A.; Frolova, I. L.; Shmikk, G. N.; Loffa, I. F. *Polym. Bull.* **1984**, *12*, 195.
(3) Hoogsteen, W.; Kormelink, H.; Eshuis, G.; ten Brinke, G.; Pennings, A. J. *J. Mater. Sci.* **1988**, *23*, 3467.
(4) Kelly, A.; Macmillan, N. H. *Strong Solids*, 3rd ed.; Oxford Science Publications, Clarendon Press: Oxford, 1986; pp 7–8.
(5) de Boer, J. H. *Trans. Faraday Soc.* **1936**, *32*, 10.
(6) He, T. *Makromol. Chem.* **1987**, *188*, 2489.
(7) Wool, R. P.; Bretzlaff, R. S.; Li, B. Y.; Wang, C. H.; Boyd, R. H. *J. Polym. Sci., Polym. Phys. Ed.* **1986**, *24*, 1039.
(8) Kausch, H. H. *Polymer Fracture, Polymers/Properties and Applications 2*; Springer-Verlag: Berlin, Heidelberg, 1987.
(9) Reneker, D. H. *J. Polym. Sci.* **1962**, *59*, S39.
(10) Mansfield, M.; Boyd, R. H. *J. Polym. Sci., Polym. Phys. Ed.* **1978**, *16*, 1227.
(11) Wahlstrand, K. J. *J. Chem. Phys.* **1985**, *82*, 5247.
(12) Reneker, D. H.; Mazur, J. *Polymer* **1983**, *24*, 1387.
(13) Reneker, D. H.; Mazur, J. *Polymer* **1988**, *29*, 3.
(14) McCullough, R. L. *J. Polym. Sci., Polym. Phys. Ed.* **1977**, *15*, 1805.
(15) McCullough, R. L.; Eisenstein, A. J.; Weikart, D. F. *J. Polym. Sci., Polym. Phys. Ed.* **1977**, *15*, 1837.
(16) Reneker, D. H.; Mazur, J. *Polymer* **1984**, *25*, 1549.
(17) GROMOS, copyright W. F. van Gunsteren and H. J. C. Berendsen; BIOMOS bv Biomolecular Software, Laboratory of Physical Chemistry, University of Groningen, Nijenborgh 16, 9747 AG Groningen, The Netherlands.
(18) Schnyder, R. G.; Schachtschneider, J. H. *Spectrochim. Acta* **1965**, *21*, 169.
(19) Weber, T. A. *J. Chem. Phys.* **1979**, *70*, 4277.
(20) van der Ploeg, P.; Berendsen, H. J. C. *J. Chem. Phys.* **1982**, *76*, 3271.
(21) Ryckaert, J. P.; Bellemans, A. *Faraday Discuss. Chem. Soc.* **1978**, *66*, 95.
(22) van Gunsteren, W. F.; Berendsen, H. J. C.; Rullmann, J. A. C. *Mol. Phys.* **1981**, *44*, 69.
(23) GROMOS manual, p II-70 (see ref 17).
(24) van Gunsteren, W. F.; Karplus, M. *J. Comput. Chem.* **1980**, *1*, 266.
(25) Courant, R. *Bull. Am. Math. Soc.* **1943**, *49*, 1.
(26) Fletcher, R.; Reeves, C. M. *Comput. J.* **1964**, 7, 149.
(27) Treloar, L. R. G. *Polymer* **1960**, *1*, 95.
(28) Sakurada, I.; Kaji, K. *J. Polym. Sci., Polym. Symp.* **1970**, *No. 31*, 57.
(29) Feldkamp, L. A.; Venkatamaran, G.; King, J. S. *Neutron Inelastic Scattering, Proceedings, Symposium on Neutron Inelastic Scattering, Copenhagen, IAEA, Vienna* **1968**, *2*, 159.
(30) Mizushima, S. I.; Shimanouchi, T. *J. Am. Chem. Soc.* **1949**, *71*, 1320.
(31) Barham, P. J.; Keller, A. *J. Polym. Sci., Polym. Phys. Ed.* **1979**, *17*, 591.
(32) Fanconi, B.; Rabolt, J. F. *J. Polym. Sci., Polym. Phys. Ed.* **1985**, *23*, 1201.
(33) Peterlin, A. *Ultra-High Modulus Polymers*; Ciferri, A., Ward, I. M., Eds.; Applied Science Publishers: England, 1979; p 279.
(34) Dijkstra, D. J.; Pennings, A. J. *Polym. Bull.* **1988**, *19*, 73.
(35) Flory, P. J.; Yoon, D. Y. *Nature* **1978**, *272*, 226.
(36) Lacher, R. C.; Bryant, J. L.; Howard, L. N.; Summers, D. W. *Macromolecules* **1986**, *19*, 2639.
(37) Smook, J.; Flintermann, M.; Pennings, A. J. *Polym. Bull.* **1980**, *2*, 775.
(38) Pennings, A. J.; Roukema, M.; van der Veen, A., to be published.
(39) Dijkstra, D. J. Ph.D. Thesis, University of Groningen.
(40) Dijkstra, D. J.; Pennings, A. J. *Polym. Bull.* **1988**, *19*, 481.
(41) Postema, A. R.; Hoogsteen, W.; Pennings, A. J. *Polym. Commun.* **1987**, *28*, 148.
(42) Dijkstra, D. J.; Pennings, A. J. *Polym. Bull.* **1987**, *17*, 507.
(43) Dijkstra, D. J.; Torfs, J. C. M.; Pennings, A. J. *Colloid Polym. Sci.*, accepted.
(44) See ref 8, p 225.
(45) Termonia, Y.; Smith, P. *Polymer* **1986**, *27*, 1845.

Registry No. Polyethylene, 9002-88-4.